

Mode-coupling analysis of atomic dynamics in liquid lead

W. Gudowski, M. Dzugotov, and K.-E. Larsson

Department of Neutron and Reactor Physics, Institute of Physics, Royal Institute of Technology, S-100 44 Stockholm, Sweden

(Received 5 June 1992; revised manuscript received 16 October 1992)

A detailed mode-coupling analysis of the atomic self-motion in liquid lead at 623 K is presented and discussed. Time-correlation functions calculated in a large-scale molecular-dynamics simulation were used to derive the relevant memory functions, which were compared with those calculated within the framework of mode-coupling theory. The mode-coupling formalism for the memory function of the velocity autocorrelation function has been extended to wave-vector-dependent memory functions. The detailed analysis of the two sets of memory functions in terms of constituent coupling modes leads to the conclusion that some assumptions incorporated in the present formulation of mode-coupling theory are of limited validity. In particular, the phenomenological form for the memory function proposed by Levesque and Verlet [Phys. Rev. A **14**, 408 (1970)] for the Lennard-Jones liquid is found to be inadequate in the case of liquid lead.

PACS number(s): 51.10.+y, 61.20.Ja, 61.25.Mv, 61.20.Ne

I. INTRODUCTION

Since the first observation of a distinct coupling effect between the motion of a tagged particle in a liquid and its environment [1], there has been intense discussion focused on the interpretation of the long-time tail displayed by the velocity-autocorrelation function (VAF) of a moving particle. The leading mechanism of this phenomenon was suggested [2] to be related to the shear modes that a moving particle of a liquid generates in its environment; these waves were assumed to interact, with a certain time delay, with the particle motion.

In this paper a comprehensive analysis of the tagged-particle dynamics in a classical simple liquid is presented. The central issue addressed here is whether the mode-coupling approach can give a satisfactory account of the results obtained from direct computer simulation on a realistic liquid model using the molecular-dynamics (MD) technique. As a test case, we have chosen a MD model of liquid lead close to its melting point which was extensively explored in our earlier studies [3]. A detailed analysis of the atomic self-motion in that liquid made in terms of the relevant memory functions is presented. The analysis involves evaluation on a quantitative level, of the contribution from particular coupling modes. To make this analysis possible, the mode-coupling formalism for the memory function of the velocity-autocorrelation function [4–8] has been extended here to calculate the wave-vector-dependent memory functions. A comparison of the memory functions calculated within the framework of that theoretical model with those directly derived from the MD simulation is presented.

II. THEORY

The theoretical approach adopted in the memory-function calculations presented here is based on the observation made by Levesque and Verlet (LV) [9] on the Lennard-Jones (LJ) system. They found that the memory

function $\Gamma(t)$ for the velocity-autocorrelation function $\Phi(t)$ can be accurately accounted for by the expression

$$\Gamma(t) = A \exp(-at^2) + Bt^4 \exp(-bt). \quad (1)$$

The underlying assumption which legitimates the above division of $\Gamma(t)$ into two terms is that these terms represent two distinct dynamical regimes in the atomic dynamics in a liquid. The first term, rapidly decaying with time, is supposed to represent the effect of a binary collision between a moving tagged particle and a fluid particle from its environment, whereas the second one incorporates a contribution from the collective processes associated with multiple collisions. The latter gives rise to the buildup of a backflow around a moving tagged particle which reacts, after a certain time delay, with the particle motion. This leads to the conclusion that the long-time behavior of $\Gamma(t)$ should be controlled by the long-wavelength transverse currents in the backflow.

In the Appendix we present, in explicit form, the equations for the memory function which were used in the analysis performed here. The binary-collision term $\Gamma^{SB}(Q, t)$ is represented by the Fokker-Planck collision function with a Gaussian ansatz [8] [see Eqs. (A4)–(A7)]. The Q dependence of the relaxation time τ_Q is given by Eq. (A6). In the original study [5], τ_0 entering that expression is determined by a short-time expansion of $\Gamma^{SB}(t)$ and application of the superposition approximation for the entering triplet distribution function $g_3(\mathbf{r}_1, \mathbf{r}_2, \mathbf{r}_3)$. Sjögren [5] found, however, that this form could not adequately describe the width of the memory function derived from the VAF's for argon and rubidium. Therefore, he changed τ_0 to fit the memory function of the VAF's. As the whole theoretical memory function then agreed with the experimental functions, this procedure can be regarded as fitting the theoretical VAF's to the measured diffusion coefficients. As this reflects the difficulties of theory in describing $\Gamma^{SB}(t)$ correctly, we derived τ_0 directly from the VAF memory function which has been simulated by MD. It is important to note that

in the small- Q region the Fokker-Planck term converges to the Gaussian ansatz. On the other hand, for large Q it approaches the free-gas memory function with a characteristic undershoot which follows the rapidly decaying part.

There are four coupling terms which are believed to provide the most significant contribution to the memory function being discussed. These include the density-

density coupling R_{00}^s , and two terms describing coupling between the density fluctuations and the longitudinal current, R_{01}^s and R_{11}^s , as well as the density-transversal-current coupling term R_{22}^s . The Q and ω dependences of these coupling terms are described by Eqs. (A8)–(A11). Finally, Γ_{11}^s , the second-order memory function of the self part of the density correlation function $\hat{F}^s(Q, \omega)$, may be expressed as

$$\hat{F}_{11}^s(Q, \omega) = \frac{\hat{F}_{11}^{sB}(Q, \omega) + \hat{R}_{00}^s(Q, \omega) + \hat{F}_{11}^{sB}(Q, \omega)\hat{R}_{01}^s(Q, \omega)}{1 - \hat{R}_{01}^s(Q, \omega) - \hat{F}_{11}^{sB}(Q, \omega)\hat{R}_{11}^s(Q, \omega) - [\hat{F}_{11}^{sB} + \hat{R}_{00}^s(Q, \omega) + \hat{F}_{11}^{sB}\hat{R}_{01}^s(Q, \omega)]\hat{R}_{22}^s(Q, \omega)}. \quad (2)$$

Here the terms marked by the index s are related to the self part of the correlation function, while the terms expressing the binary-collision part are denoted by the index B . Using a reasonable approximation, the last equation can be rewritten in the following form:

$$\begin{aligned} \hat{F}_{11}^s(Q, \omega) &= \hat{F}_{11}^{sB}(Q, \omega) + \hat{R}_{00}^s(Q, \omega) + 2\hat{F}_{11}^{sB}(Q, \omega)\hat{R}_{01}^s(Q, \omega) + [\hat{F}_{11}^{sB}(Q, \omega)]^2\hat{R}_{11}^s(Q, \omega) \\ &+ \hat{F}_{11}^{sB}[\hat{F}_{11}^{sB} + \hat{R}_{00}^s(Q, \omega) + \hat{F}_{11}^{sB}\hat{R}_{01}^s(Q, \omega)]\hat{R}_{22}^s(Q, \omega) = \hat{F}_{11}^{sB} + \hat{F}_{00}^R + \hat{F}_{01}^R + \hat{F}_{11}^R + \hat{F}_{22}^R, \end{aligned} \quad (3)$$

where the terms describing recollision events are marked by the index R .

For the discussion that follows, it is worthwhile to mention two important asymptotic relations describing behavior of the Q -dependent memory functions in the long-wavelength limit:

$$\hat{D}(Q \rightarrow 0, \omega) \rightarrow V_0^2 \hat{\Phi}(\omega), \quad (4)$$

$$\hat{F}_{11}^s(Q \rightarrow 0, \omega) \rightarrow \hat{F}(\omega), \quad (5)$$

where $\hat{\Phi}(\omega)$ and $\hat{F}(\omega)$ are frequency spectra of the VAF and its memory function, respectively, and $V_0^2 = k_B T/m$, m being the particle mass.

The coupling terms for $Q=0$ were calculated using Eqs. (A17)–(A20), thus avoiding the singularities embedded in Eqs. (A8)–(A11). This approach also provides an opportunity to crosscheck the calculations of the Q -dependent coupling terms which, in the long-wavelength limit, have to converge to the values indicated in Eqs. (4) and (5).

III. MOLECULAR-DYNAMICS SIMULATION

As can be seen from Eqs. (A8)–(A11), the input information required to calculate the coupling terms discussed above involves several space-time correlation functions. These include the density-correlation function $F(Q, t)$, its self part $F^s(Q, t)$, and the longitudinal-current correlation function $C_1(Q, t)$ as well as the transversal-current correlation function $C_t(Q, t)$. Besides these dynamical characteristics, adequate information on the structure of the simulated liquid was needed in the form of its structure factor $S(Q)$ and the corresponding pair-distribution function $g(r)$. In this study, the above-listed functions were derived from the MD simulation of liquid lead which was carried out at $T=623$ K and the corresponding observable density. The model was comprised of 16 384 particles interacting via the effective pair interionic potential [10]. This model has been extensively explored in our

earlier studies of liquid lead [3]. Its structure and the dynamical properties were found to agree, within the experimental accuracy limits, with those measured by neutron scattering on the real liquid lead [11]. Therefore, the analysis of the atomic dynamics in liquid lead reported here using the above model should be regarded as an extension of the experimental information on this system available to the area that is inaccessible by existing experimental methods.

The correlation functions listed above were simulated in the wave-vectors domain ranging from $Q=0.07$ to 6.0 \AA^{-1} . The crucial advantage of the large-size MD system employed was that it allowed adequate exploration of the important long-wavelength region. In order to avoid unnecessary Fourier transformations, we derived the memory function for the tagged-particle motion from the corresponding source correlation function in the time domain where the latter function was produced by the MD simulation. This was done by solving numerically [12] the integro-differential equations corresponding to Eqs. (A1) and (A2):

$$\frac{\partial F_s(Q, t)}{\partial t} = - \int_0^t dt' Q^2 D(Q, t-t') F_s(Q, t'), \quad (6)$$

$$\frac{\partial D(Q, t)}{\partial t} = - V_0^2 \int_0^t dt' \Gamma^s(Q, t-t') D(Q, t'). \quad (7)$$

The numerical differentiation involved imposes strict requirements regarding the acceptable level of statistical noise in the input MD-generated correlation functions. In this respect, the use of a large MD system is also of crucial advantage. The estimated level of statistical noise in the simulated $F^s(Q, t)$ was found to be well below 1%.

IV. MEMORY FUNCTIONS

The general view of the memory function $D(Q, t)$ derived from the MD-simulated tagged-particle density-correlation function $F^s(Q, t)$ using Eq. (6) and its frequen-

cy spectrum is shown in Fig. 1. In the long-wavelength limit, $D(Q, t)$ converges smoothly to a VAF (shown by the dashed line) which is a direct result of the MD simulation. This demonstrates agreement with the asymptotic relation (4), and it may be regarded as an important test of consistency in the memory-function calculation routine. An interesting feature of the function $D(Q, t)$ presented is that the time corresponding to its first minimum is practically Q invariant; this time is about 0.26 ps. As Q grows, the minimum becomes less pronounced, until it disappears at about $Q = 5 \text{ \AA}^{-1}$. The first minimum is followed by oscillations which are well developed at the lowest Q explored here; for higher values of Q , the oscillations are considerably smeared out.

The normalized second-order memory function $\Gamma_{11}^s(Q, t)$ and its spectrum $\Gamma_{11}^s(Q, \omega)$, which are also shown in Fig. 1, demonstrate general consistency with the LV form [Eq. (1)]. This implies the presence of sizable mode coupling effects. The function can be easily decomposed into two parts: the rapidly decaying part of Gaussian-like form and the one varying much more slowly with time, which stretches out to 2 ps. The amplitude of the latter component decreases with an increase in Q . In the corresponding spectral presentation, that slowly decaying component gives rise to a sharp low-frequency peak which superimposes the Gaussian-like spectrum produced by the rapidly decaying part of $\Gamma_{11}^s(Q, t)$. The distinct minimum separating the two parts of $\Gamma_{11}^s(Q, t)$ described becomes more pronounced with growing Q , apparently converging to the free-gas memory-function limit. Similar behavior is demonstrated by the VAF memory function $\Gamma(t)$, which is also shown in Fig. 1 by the dashed curve. An interesting observation is that the memory functions $D(Q, t)$ and $\Gamma_{11}^s(Q, t)$ demonstrate very small variation with respect to Q within the Q range where the

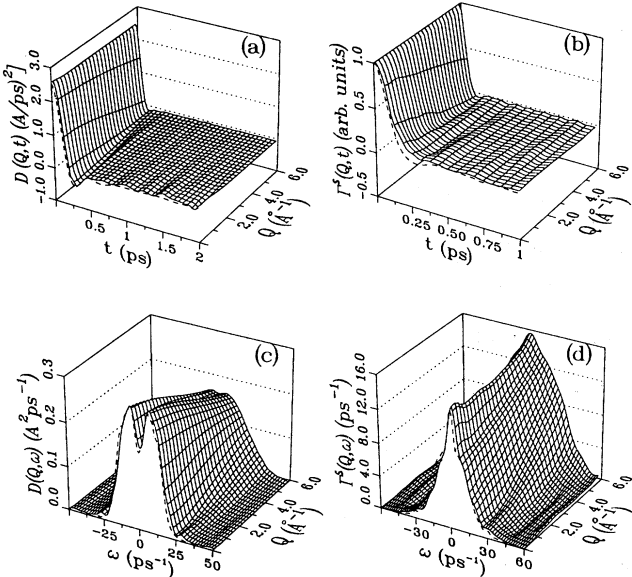


FIG. 1. Memory functions of the MD-simulated $F^s(Q, t)$: (a) $D(Q, t)$; (c) its frequency spectrum $D(Q, \omega)$; (b) $\Gamma^s(Q, t)$; and (d) its frequency spectrum $\Gamma^s(Q, \omega)$.

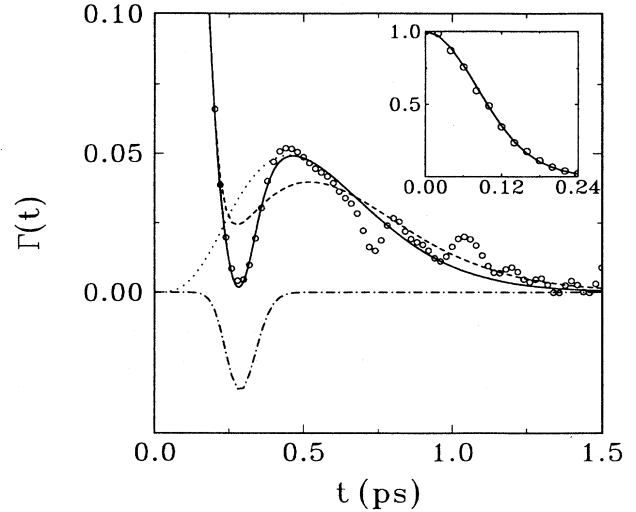


FIG. 2. Open circles, the VAF memory function $\Gamma(t)$; dashed line, the best fit using the LV form [Eq. (1)] with the following values of parameters: $A = 109.2$, $a = 73.4$, $B = 3224$, and $b = 7.68$. The solid line shows the best fit using Eq. (9) with parameters $A = 109.2$, $a = 73.7$, $B = 7313$, $b = 8.9$, $C = -1.5 \times 10^{11}$, $c = 84.2$, and $\gamma = 14$; dotted line, the term in Eq. (9) containing t^4 ; dash-dotted line, the additional negative term in Eq. (9).

relaxation time for $F^s(Q, t)$ varies by two orders of magnitude.

The two components of the memory functions described are separated by a deep valleylike minimum. This detail cannot be reproduced by the LV expression (1). Figure 2 shows the best fit to $\Gamma(t)$ obtained by varying the parameters entering (1). The fit clearly fails to reproduce the minimum. We found that one possibility to improve the agreement is to introduce an additional term with a negative amplitude. This might be of physical significance and will be discussed later. The above-described failure of the LV form for memory function when tested against the MD results has a very important consequence for the mode-coupling analysis.

V. MODE-COUPLING ANALYSIS

Since the rapidly decaying part of $\Gamma_{11}^s(Q, t)$ can be approximated by a Gaussian, it is convenient to describe its time decay in terms of the relaxation time τ_Q , defined as

$$\Gamma_{11}^s(Q, t = \tau_Q) = \frac{1}{e} \Gamma_{11}^s(Q, t = 0) \quad (8)$$

In Fig. 3, τ_Q for the memory function $\Gamma_{11}^s(Q, t)$ directly derived from the MD results is compared with that obtained from mode-coupling analysis and the one used in the Gaussian ansatz [see Eq. (A6)]. The three sets of data seem to be in good agreement. The small discrepancy between the MD results and those calculated using the mode-coupling approach, which looks like a parallel shift, can be easily accounted for by the uncertainty originated from the finite time step used in the MD simula-

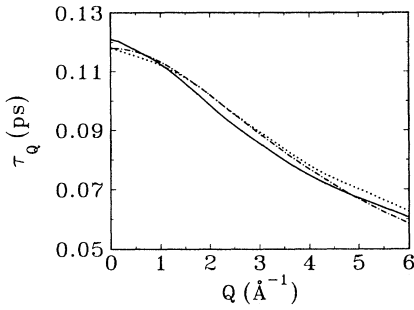


FIG. 3. Relaxation time for $\Gamma_{11}^s(Q, t)$ as a function of Q . Dotted line, MD-simulated results; solid line, mode-coupling calculation; dash-dotted line, Gaussian ansatz $M^s(Q, t)$ as given in Eq. (A6).

tion. However, this agreement does not constitute any proof that the mode-coupling theory is correct. It confirms only that the approximation concerning the binary part of the self-correlation functions up to t values close to τ_Q is reasonable. Figure 3 also shows that the Gaussian ansatz $M^s(Q, t)$ in Eq. (A6) describes the MD results very well for the Q values below 4 \AA^{-1} . For the larger wave vectors, in the region where free-particle behavior begins to dominate, the MD curve is converging to that predicted by the mode-coupling model.

The coupling terms Γ_{00}^R , Γ_{01}^R , Γ_{11}^R and Γ_{22}^R calculated using Eq. (A7)–(A11) are presented in Fig. 4. In the long-wavelength limit, these terms converge smoothly to those derived from the VAF memory function, which are shown by the dashed line at $Q=0$. The latter were calcu-

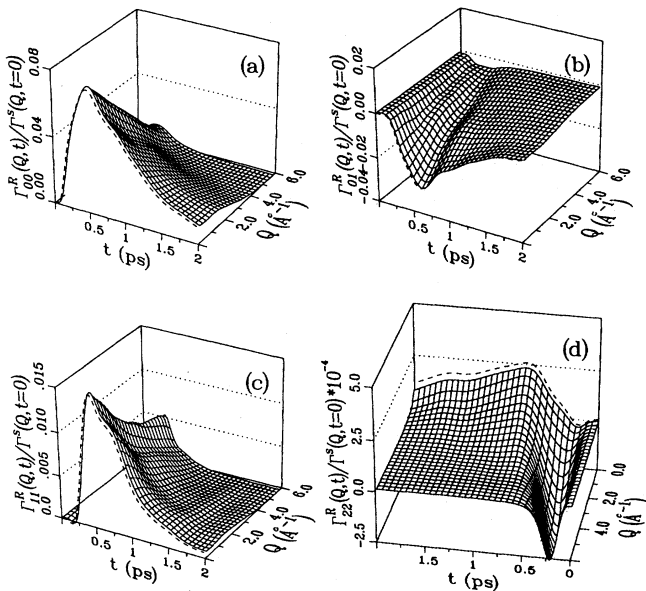


FIG. 4. Recollision terms of $\Gamma_{ij}^s(Q, t)$ calculated according to mode-coupling theory [Eq. (3)]. The dashed lines at $Q=0$ represent the corresponding calculation for the VAF memory function using Eqs. (A17)–(A20).

lated using Eqs. (A17)–(A20), as mentioned above. This asymptotic behavior is an important consistency test for the numerical procedure we employed here. In Fig. 5 we compare the mode-coupling-theory results on Γ^s with those derived from the MD-simulated $F^s(Q, t)$. In the insets, the difference between these two memory functions is presented, compared with contributions from the above coupling terms. The curves shown for $Q=0$ correspond to the VAF memory function. All four of these VAF coupling terms look similar to those obtained for the LJ liquid [8]. The comparison of the two memory functions presented demonstrates that there is a considerable discrepancy between the MD results and those calculated within the framework of mode-coupling theory. The important observation here is that mode-coupling theory overestimates the coupling effect by approximately a factor of 2 within the Q range below 6 \AA^{-1} . Moreover, the dip separating the binary part and the mode-coupling part in the low- Q limit is irreproducible by the theory. As we suggested above, this particular feature of the memory function seems to be inherited from the LV assumption [Eq. (1)].

A similar comparison for the memory function $D(Q, t)$ presented in Fig. 6 also demonstrates a perceptible discrepancy between the two sets of results. The mode-coupling theory curves, as compared with those derived from MD, overestimate the negative part of this memory function for $Q=0$ and underestimate this part for large- Q values. For $Q=2.25$, which corresponds to the position of the main peak of $S(Q)$, the mode-coupling-theory curve exhibits an unstructured negative long-time tail deviating significantly from the corresponding MD curve. It is important to note that in order to calculate $D(Q, t)$, only the first derivative of the MD-simulated correlation function $F^s(Q, t)$ is needed, as compared with the third derivative required to calculate $F_{11}^s(Q, t)$ [13]. Therefore, the latter is expected to contain a much higher level of noise. At the same time, both of these memory functions derived from the MD data exhibit approximately the same level of noise, as can be estimated from the curves presented. This indicates that the level of noise introduced by the numerical routine employed to derive the memory functions is very small compared with that which results from the statistical uncertainty in the original MD-simulated $F^s(Q, t)$.

Traditionally, self-motion of particles in a liquid used to be analyzed in terms of reduced half-width of $S^s(Q, \omega)$, $\Delta(Q) = \omega_{1/2}(Q)/DQ^2$, D being the self-diffusion coefficient, and the reduced amplitude of its peak

$$\Sigma(Q) = \pi D Q^2 S^s(Q, \omega=0).$$

In our MD model, $D = 1.82 \times 10^{-5} \text{ cm}^2/\text{s}$ [10], which is in good agreement with the experimental value. In Fig. 7 the results on $\Delta(Q)$ and $\Sigma(Q)$ calculated for the MD-simulated $F^s(Q, t)$ are compared with those calculated using the mode-coupling approach. In the same figure, we also present the results for the binary part F^{sB} . The comparison of these results clearly demonstrates that the mode-coupling theory limited to the four coupling terms as described above fails to reproduce the MD results.

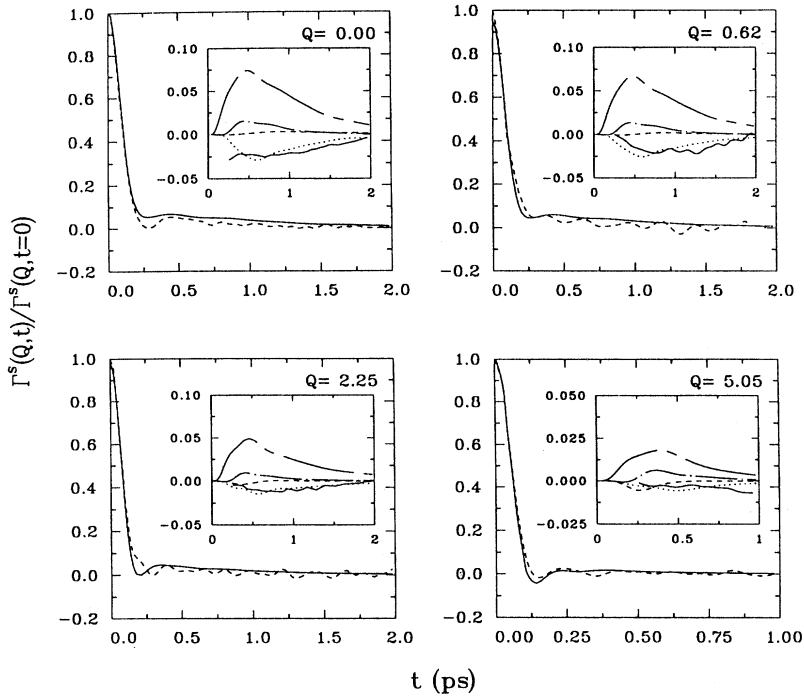


FIG. 5. Solid line, the memory function $\Gamma_{11}^s(Q, t)$ calculated according to mode-coupling theory; dashed line, the same function derived directly from MD simulation. The insets present the contributions from the recollision terms: short-dashed line, $\Gamma_{00}^R(Q, t)$; dotted line, $\Gamma_{01}^R(Q, t)$; dash-dotted line, $\Gamma_{11}^R(Q, t)$; long-dashed line, $\Gamma_{22}^R(Q, t)$. The solid line in the insets shows the difference between the two memory-function calculations (the curve was smoothed to remove statistical noise).

The self-diffusion coefficient, which is the limit of $1/\Sigma(Q)$ for $Q \rightarrow 0$, is underestimated by the theory by more than 30%, and the estimated small- Q limit of $\Delta(Q)$ comes out to be about 25% too low. This discrepancy is a direct consequence of the fact that the theory overestimates the coupling terms, as shown in Fig. 5.

VI. DISCUSSION

The detailed quantitative analysis in terms of memory functions presented above indicates that the simulated

atomic dynamics in liquid lead significantly deviate from what is predicted by the mode-coupling theory. The theory, as formulated by Sjögren and Sjölander [4], is essentially based on the LV empirical form for memory function as described by Eq. (1). This form was found to be valid for the system simulated using the LJ potential. According to Sjögren [7], the same general form can also describe the memory function $\Gamma(t)$ in the case of liquid rubidium. The most characteristic feature predicted by Eq. (1) is that the recollision part of $\Gamma(t)$ begins as t^4 . As we have shown in Fig. 2, in the case of liquid lead studied

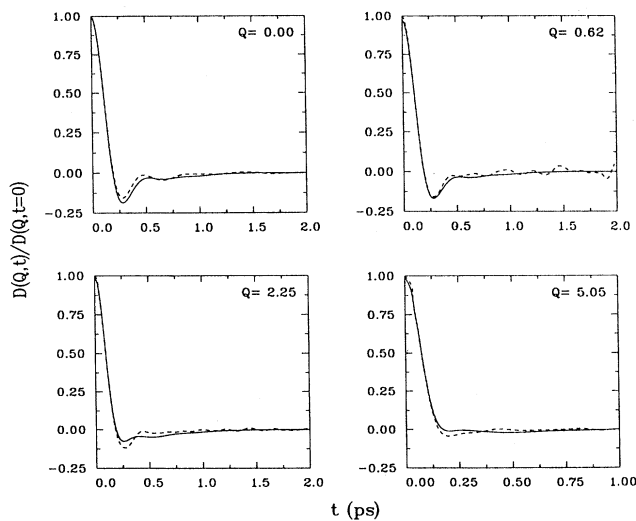


FIG. 6. Normalized memory functions $D(Q, t)$ calculated according to mode-coupling theory (solid line) compared with that derived from MD simulation (dashed line) for chosen Q values.

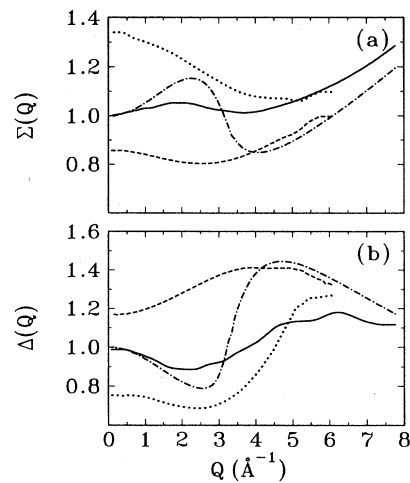


FIG. 7. (a) $\Sigma(Q)$, reduced peak value and (b) $\Delta(Q)$, reduced half-width of $S^s(Q, \omega)$. Solid line, MD results; dashed line, mode-coupling calculation; dotted line, the binary part, $\hat{F}^{SB}(Q, \omega)$; dashed-dotted line, results of the alternative mode-coupling approach of Götze-Zippelius-Lorenz [14].

here, Eq. (1) fails to describe the MD-simulated VAF memory function $\Gamma(t)$. In order to improve the fit, we tried to modify the LV expression (1) by introducing an additional negative term:

$$\Gamma(t) = A \exp(-at^2) + Bt^4 \exp(-bt) - Ct^\gamma \exp(-c^2 t^2). \quad (9)$$

A fit to the simulated memory function using this functional form is shown in Fig. 2. The first term in this fit has not changed and the second term has only increased the amplitude as compared with the previous fit using form (1). At the same time, addition of a negative term with $\gamma = 14$ provides a very good description of the deep minimum separating the two parts of the memory function. It should be noted that the additional negative component in question occurs in the time window which partly covers both the Gaussian-like part and the long-time tail of the memory function. The existence of this component suggests several conclusions which might have the following serious implications regarding some basic points of mode-coupling theory in its present form.

(i) If added to the first term in the LV form, this would mean that the so-called binary-collision term has to be thoroughly reformulated. This suggestion does not seem unreasonable; indeed, in the case of continuous long-range potential, the short-time interaction of a particle with its neighbors is a many-body process which cannot be universally and adequately described in terms of binary collisions.

(ii) Among the mode-coupling terms discussed above, it is $\Gamma_{00}^R(Q, t)$ describing coupling between density fluctuations and self-motion which starts as t^4 . This is the leading structural element in the present formulation of the theory aimed at forcing the recollision term of $\Gamma(t)$ to start as t^4 in agreement with the LV empirical form (1). This may not be a valid argument in the case of liquid lead.

(iii) The time window where the new term introduced in Eq. (9) gives a considerable contribution to the memory function overlaps with both the "binary"-collision part and the recollision part as formulated by the present theory (see Fig. 2). This might be regarded as an indication that a coupling between these two domains cannot be neglected, at least in the case of liquid lead.

The present formulation of the theory is based upon the subtraction of the free-gas function $F^0(Q, t)$ from $F^s(Q, t)$ in the calculation of the coupling terms aimed at getting rid of the t^2 expansion term which instead appear in the Gaussian term. This construction worked reasonably well for the LJ liquid and for liquid rubidium. However, even in those cases, the half-width of the binary component had to be adjusted in order to obtain the correct value of the diffusion constant [5]. For liquid lead, comparison of half-widths and peak values of the simulated $S^s(Q, \omega)$ with those predicted by the Sjögren-Sjölander formulation of the theory, as well as by the Götze-Zipellius-Lorenz formulation [14] (Fig. 7), shows that both formulations fail to quantitatively describe the simulation results.

In order to see why the short-time-scale atomic dynam-

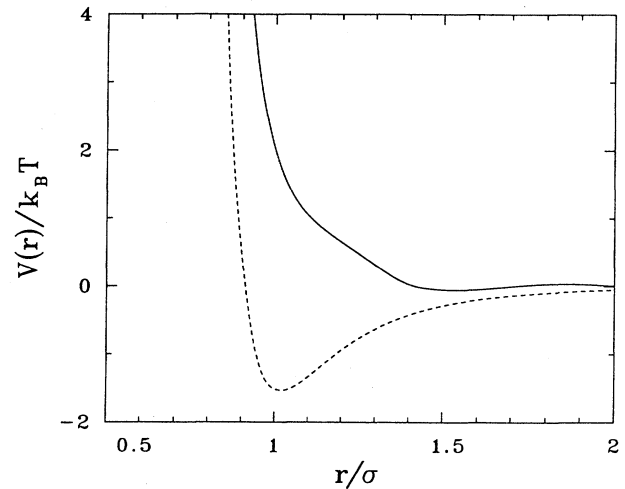


FIG. 8. Pair potential for liquid lead applied in this study (solid line) compared with the Lennard-Jones potential (dashed line). The unit of distance is the effective atomic diameter, that is, the position of the first peak of $g(r)$ in the corresponding liquid.

ics in liquid lead is significantly different from that in the LJ liquid, we have to compare the corresponding pair potentials in these two liquids (see Fig. 8). The fundamental distinction between the two is that while the LJ potential has a pronounced minimum at the position of the first neighbor, the pair potential in liquid lead is positive and strongly repulsive at that distance. Therefore, the atomic dynamics in the LJ liquid might be expected to have a short-time component corresponding to the free particle behavior, whereas in liquid lead a single-particle motion is coupled with the motions of its neighbors at any time scale. This argumentation is consistent with the fact that the theory in its present formulation was successful in describing the memory function in liquid rubidium where the pair potential also has a minimum at the nearest-neighbor distance. The analysis presented suggests that in the case of liquid lead the binary-collision approach to the description of the short-time part of the memory function has to be reformulated. Also, the idea of subtracting the free-gas term from $F^s(Q, t)$ we discussed above becomes dubious in this case.

VII. CONCLUDING REMARKS

In summary, we presented a detailed mode-coupling analysis of atomic self-motion in a realistic MD model of liquid lead. The relevant memory functions and constituent mode-coupling terms were derived from the simulated correlation functions and compared with the corresponding mode-coupling-theory predictions. The main conclusion of this study is that some assumptions incorporated in the present formulation of the theory, which used to be regarded as universal are, in fact, of limited validity. In particular, the LV form (1) of the memory function derived for the LJ liquid was demonstrated to be inadequate for the memory functions derived here for the model of liquid lead. This is concluded to be related to

the particular form of pair potential utilized in this model. In the light of the analysis presented, the universality of other basic postulates incorporated in the theory, such as, for instance, the concept of binary collision, is also questioned. The question still remains as to whether the theory can be formulated in such a way that it would be able to account for all possible variations in atomic dynamics in simple liquids caused by different forms of pair potential.

ACKNOWLEDGMENTS

We are grateful to Professor A. Sjölander and Dr. L. Sjögren for providing an explicit form of the mode-coupling equations and for very fruitful discussions. One of us (M.D.) acknowledges support from the Swedish Natural Research Foundation.

APPENDIX

Memory-function equations relate the density-self-correlation function $\hat{F}^s(Q, \omega)$ with its memory functions

$$\hat{\Gamma}_{11}^s(Q, \omega) = \frac{\hat{\Gamma}_{11}^{sB}(Q, \omega) + \hat{R}_{00}^s(Q, \omega) + \hat{\Gamma}_{11}^{sB}(Q, \omega) \hat{R}_{01}^s(Q, \omega)}{1 - \hat{R}_{01}^s(Q, \omega) - \hat{\Gamma}_{11}^{sB}(Q, \omega) \hat{R}_{11}^s(Q, \omega) - [\hat{\Gamma}_{11}^{sB} + \hat{R}_{00}^s(Q, \omega) + \hat{\Gamma}_{11}^{sB} \hat{R}_{01}^s(Q, \omega)] \hat{R}_{22}^s(Q, \omega)}. \quad (\text{A3})$$

The binary-collision term Γ^{sB} is respected by a Fokker-Planck collision term with a Gaussian ansatz M^s :

$$\omega_E \hat{F}^{sB}(Q, \omega) = \frac{1}{\omega_E \hat{M}^s(Q, \omega)} \frac{1}{\rho} \left[1 + \sum_{n=1}^{\infty} \frac{(k^2)^n}{(\rho+1) \cdots (\rho+n)} \right], \quad (\text{A4})$$

where

$$k^2 = \frac{Q^2/m\beta\omega_E^2}{[\omega_E \hat{M}^s(Q, \omega)]^2}, \quad \rho = k^2 - i \frac{\omega/\omega_E}{\omega_E \hat{M}^s(Q, \omega)}, \quad (\text{A5})$$

$$M^s(Q, t) = e^{-(t/\tau_Q)^2}, \quad \tau_Q = \frac{\tau_0}{\left[1 + \frac{5}{2} \frac{\tau_0^2}{m\beta} Q^2 \right]}, \quad (\text{A6})$$

and

$$\hat{\Gamma}_{11}^{sB}(Q, \omega) = \omega_E \left\{ \frac{Q^2}{m\beta\omega_E^2} \frac{[\omega_E \hat{F}^{sB}(Q, \omega)]}{1 + i \frac{\omega}{\omega_E} [\omega_E \hat{F}^{sB}(Q, \omega)]} + i \frac{\omega}{\omega_E} \right\}. \quad (\text{A7})$$

Finally, the mode-coupling terms are given by the equations

$$\hat{R}_{00}^s(Q, \omega) = \frac{\omega_E}{16\pi^2} \frac{V_0^2 Q_0^5}{n\omega_E^2} \left\{ \frac{1}{Q^3} \int_0^\infty dQ' Q' \left[1 - \frac{1}{S(Q')} \right]^2 \right. \\ \left. \times \int_{|Q'-Q|}^{Q'+Q} dk k (Q^2 + Q'^2 - k^2)^2 \int_0^\infty d\tau e^{i\omega\tau} [F^s(k, \tau/\omega_E) - F^0(k, \tau/\omega_E)] F(Q', \tau/\omega_E) \right\}, \quad \tau = \omega_E t \quad (\text{A8})$$

$$\hat{R}_{01}^s(Q, \omega) = \frac{1}{16\pi^2} \frac{Q_0^3}{n} \left\{ \frac{1}{Q^3} \int_0^\infty \frac{dQ'}{Q'} \left[1 - \frac{1}{S(Q')} \right] t_l(Q') \right. \\ \left. \times \int_{|Q'-Q|}^{Q'+Q} dk k (Q^2 + Q'^2 - k^2)^2 \int_0^\infty d\tau e^{i\omega\tau} [F^s(k, \tau/\omega_E) - F^0(k, \tau/\omega_E)] \frac{\partial F(Q', t)}{\partial t} \right\}, \quad t = \frac{\tau}{\omega_E} \quad (\text{A9})$$

$\hat{D}(Q, \omega)$ and $\hat{\Gamma}_{11}^s(Q, \omega)$:

$$\hat{F}^s(Q, \omega) = \frac{1}{-i\omega + \frac{Q^2/m\beta}{-i\omega + \hat{\Gamma}_{11}^s(Q, \omega)}} \\ = \frac{1}{-i\omega + Q^2 \hat{D}(Q, \omega)}, \quad (\text{A1})$$

where m is the particle mass and $\beta = 1/k_B T$. The same relation can be written for the binary part of the density-self-correlation function

$$\hat{F}^{sB}(Q, \omega) = \frac{1}{-i\omega + \frac{Q^2/m\beta}{-i\omega + \hat{\Gamma}_{11}^{sB}(Q, \omega)}} \\ = \frac{1}{-i\omega + Q^2 \hat{D}_B(Q, \omega)}. \quad (\text{A2})$$

The memory function $\hat{\Gamma}_{11}^s(Q, \omega)$ is calculated in mode-coupling theory by the following equation:

$$\hat{R}_{11}^s(Q, \omega) + \frac{1}{\omega_E} \frac{1}{16\pi^2} \frac{Q_0^3}{n} \left\{ \frac{1}{Q^3} \int_0^\infty \frac{dQ'}{Q'} [t_l(Q')]^2 \right. \\ \left. \times \int_{|Q'-Q|}^{Q'+Q} dk k (Q^2 + Q'^2 - k^2)^2 \int_0^\infty d\tau e^{i\omega\tau} [F^s(k, \tau/\omega_E) - F^0(k, \tau/\omega_E)] C_l \left[Q', \frac{\tau}{\omega_E} \right] \right\}, \quad (\text{A10})$$

$$\hat{R}_{11}^s(Q, \omega) + \frac{1}{\omega_E} \frac{1}{16\pi^2} \frac{Q_0^3}{n} \left\{ \frac{1}{Q^3} \int_0^\infty \frac{dQ'}{Q'} [t_{tr}(Q')]^2 \int_{|Q'-Q|}^{Q'+Q} dk k [4Q^2 Q'^2 - (Q^2 + Q'^2 - k^2)^2] \right. \\ \left. \times \int_0^\infty d\tau e^{i\omega\tau} [F^s(k, \tau/\omega_E) - F^0(k, \tau/\omega_E)] C_l \left[Q', \frac{\tau}{\omega_E} \right] \right\}. \quad (\text{A11})$$

Q is given in units of Q_0 and ω in units of ω_E , where Q_0 is the position of the main peak of $S(Q)$ and ω_E is the Einstein frequency, $S(Q)$ the structure factor, $C_l(Q, t)$ the longitudinal-current correlation function, $C_t(Q, t)$ the transversal-current correlation function, $V_0^2 = (\beta m)^{-1}$, and

$$F^0 \left[Q, \frac{\tau}{\omega_E} \right] = \exp \left[-\frac{Q^2}{m\beta\omega_E^2} \frac{\tau^2}{2} \right] \quad (\text{A12})$$

is the free-particle density-self-correlation function

$$t_l(Q) = \frac{1}{\omega_E^2} \gamma_d^{lr}(Q) = -\frac{4\pi}{2} \left[\frac{n}{m\omega_E^2 Q_0} \right] \int_0^\infty dr r^2 g(r) \left[V''(r) + 2 \frac{V'(r)}{r} \right] \frac{\sin(Qr)}{Qr} - \frac{1}{2\omega_E^2} \gamma_d^l(Q), \quad (\text{A13})$$

$$t_l(Q) = \frac{1}{\omega_E^2} \gamma_d^l(Q) + \frac{Q_0^2}{\beta m \omega_E^2} Q^2 \left[1 - \frac{1}{S(Q)} \right], \quad (\text{A14})$$

where

$$\frac{1}{\omega_E^2} \gamma_d^l(Q) = -4\pi \left[\frac{n}{m\omega_E^2 Q_0} \right] \int_0^\infty dr r^2 g(r) \left[\frac{V'(r)}{r} \frac{\sin(Qr)}{Qr} + \left[V'(r) - \frac{V'(r)}{r} \right] \alpha_l(Qr) \right], \quad (\text{A15})$$

$$\alpha_l(Qr) = \frac{2}{(Qr)^2} \cos(Qr) - \left[\frac{2}{(Qr)^2} - 1 \right] \frac{\sin(Qr)}{Qr}, \quad (\text{A16})$$

and the index d denotes the distinct part. Values for mode-coupling terms for $Q=0$ are more easily obtained from

$$\hat{R}_{00}^s(0, \omega) = \frac{\omega_E}{6\pi^2} \frac{V_0^2 Q_0^5}{n \omega_E^2} \int_0^\infty dQ' Q'^4 \left[1 - \frac{1}{S(Q')} \right]^2 \int_0^\infty d\tau e^{i\omega\tau} [F^s(Q, \tau/\omega_E) - F^0(Q', \tau/\omega_E)] F(Q', \tau/\omega_E), \quad (\text{A17})$$

$$\hat{R}_{01}^s(0, \omega) = \frac{1}{6\pi^2} \frac{Q_0^3}{n} \int_0^\infty dQ' Q'^2 \left[1 - \frac{1}{S(Q')} \right] t_l(Q') \int_0^\infty d\tau e^{i\omega\tau} [F^s(Q', \tau/\omega_E) - F^0(Q', \tau/\omega_E)] \left[\frac{\partial F(Q', t)}{\partial t} \right], \quad t = \frac{\tau}{\omega_E}, \quad (\text{A18})$$

$$\hat{R}_{11}^s(0, \omega) = \frac{1}{\omega_E} \frac{1}{6\pi^2} \frac{Q_0^3}{n} \int_0^\infty dQ' Q'^2 [t_l(Q')]^2 \int_0^\infty d\tau e^{i\omega\tau} [F^s(Q', \tau/\omega_E) - F^0(Q', \tau/\omega_E)] C_l \left[Q', \frac{\tau}{\omega_E} \right], \quad (\text{A19})$$

$$\hat{R}_{22}^s(0, \omega) = \frac{1}{\omega_E} \frac{1}{3\pi^2} \frac{Q_0^3}{n} \int_0^\infty dQ' Q'^2 [t_{tr}(Q')]^2 \int_0^\infty d\tau e^{i\omega\tau} [F^s(Q', \tau/\omega_E) - F^0(Q', \tau/\omega_E)] C_t \left[Q', \frac{\tau}{\omega_E} \right]. \quad (\text{A20})$$

- [1] B. J. Alder and T. E. Wainright, *Phys. Rev. A* **1**, 18 (1970); W. E. Alley and B. J. Alder, *ibid.* **27**, 3158 (1983).
 [2] J. R. Dorfman and E. G. D. Cohen, *Phys. Rev. A* **6**, 776 (1972); M. de Schepper and M. H. Ernst, *Physica A* **98**, 189 (1979); J. Bosse, W. Götze, and M. Lücke, *Phys. Rev. A* **20**, 1603 (1979).

- [3] K.-E. Larsson, M. Dzugutov, and W. Gudowski, *Nuovo Cimento* **12**, 559 (1990).
 [4] L. Sjögren and A. Sjölander, *J. Phys. C* **12**, 4369 (1979).
 [5] L. Sjögren, *J. Phys. C* **13**, 705 (1980).
 [6] L. Sjögren, *Phys. Rev. A* **22**, 2866 (1980).
 [7] L. Sjögren, *Phys. Rev. A* **22**, 2883 (1980).

- [8] G. Wahnström and L. Sjögren, *J. Phys. C* **15**, 401 (1982).
- [9] D. Levesque and L. Verlet, *Phys. Rev. A* **14**, 408 (1970).
- [10] M. Dzugutov, K.-E. Larsson, and I. Ebbsjö, *Phys. Rev. A* **38**, 3609 (1988).
- [11] O. Söderström, *Phys. Rev. A* **23**, 785 (1981); U. Dahlborg, M. Davidovic, and K.-E. Larsson, *Phys. Chem. Liq.* **6**, 1033 (1985).
- [12] O. Söderström, U. Dahlborg, and W. Gudowski, *J. Phys. F* **15**, L23 (1985).
- [13] K.-E. Larsson and W. Gudowski, *Phys. Rev. A* **33**, 1968 (1986).
- [14] W. Götze and A. Zippelius, *Phys. Rev. A* **14**, 1842 (1976).
J. Lorenz, Diplomarbeit, Technische Universität München (1980).